The European Union's Copernicus Sentinel 5 Precursor (S5p) satellite in orbit.

TROPOMI: A Revolutionary New Satellite Instrument Measuring NO_2 Air Pollution

by Daniel L. Goldberg, Susan C. Anenberg, Gaige Hunter Kerr, Zifeng Lu, and David G. Streets

An overview of the Tropospheric Monitoring Instrument (TROPOMI) satellite, which demonstrates enhanced technical capabilities in the observation of nitrogen dioxide (NO_2) air pollution from space.

Nitrogen oxides (NOx = NO + NO_2) are a critical participant in the formation of ozone (O_3) and particulate matter (PM) in urban areas. NOx is also noted for its own damaging effects, including its contribution to acid rain,[1] premature aging of lungs,[2,3] and premature mortality.[4] Observing the spatial extent of NO_2 air pollution is an important first step in quantifying NOx emission rates and human exposures. Satellite data can add value to the existing ground-based monitoring network by providing pollution estimates in the areas between monitors. This article documents the capabilities of a new satellite instrument, the Tropospheric Monitoring Instrument (TROPOMI), which demonstrates enhanced technical capabilities as compared to predecessor instruments.

TROPOMI is a passive spectrometer orbiting approximately 825 km (~500 miles) above the Earth's surface as part of the European Union's Copernicus Sentinel 5 Precursor (S5p) satellite mission.[5,6] It was launched on October 13, 2017, and its dimensions are 1.4 m × 0.65 m × 0.75 m, approximately the size of large bookcase, and weighs 900 kg. TROPOMI passively observes sunlight radiation reflected back to space by the Earth's surface and atmosphere in order to calculate the amount of NO_2 in the atmospheric column. The algorithm is able to calculate NO_2 by taking a difference between a theoretical reflectance with no NO_2 pollution and the actual reflectance; the difference is equivalent to the radiation absorbed by NO_2 in the atmosphere. TROPOMI pixel sizes are 3.5 × 5.6 km^2, and the instrument observes the atmosphere globally once daily at approximately 13:30 local time. Overlapping pixel measurements over many days can be aggregated together and averaged to finer spatial resolution, such as 1 × 1 km^2; this process is called oversampling.[7] The TROPOMI S5p satellite mission follows in the successful footsteps of the NASA Aura Ozone Monitoring Instrument (OMI)[8] and Global Ozone Monitoring Experiment (GOME)[9] satellite missions. Most notably, TROPOMI has ~16x higher spatial resolution than OMI (launched 2004) and ~650x higher spatial resolution than GOME (launched 1995).

The Unprecedented Sensitivity of TROPOMI

TROPOMI, when averaged over multiple days, can differentiate the fine-scale spatial heterogeneities in urban areas,[10] such as emissions related to airport/shipping operations and high traffic, and the small spatial extent of emission sources in rural areas, such as power plants, mining operations, and wildfires. When visually inspecting the continental U.S. TROPOMI NO_2 average during the initial 20 months of the TROPOMI record (May 1, 2018–Dec 31, 2019), we see the clear spatial heterogeneity of NO_2 pollution across the United States (see Figure 1). The largest U.S. cities can be seen, and their concentration magnitudes can be compared to each other.

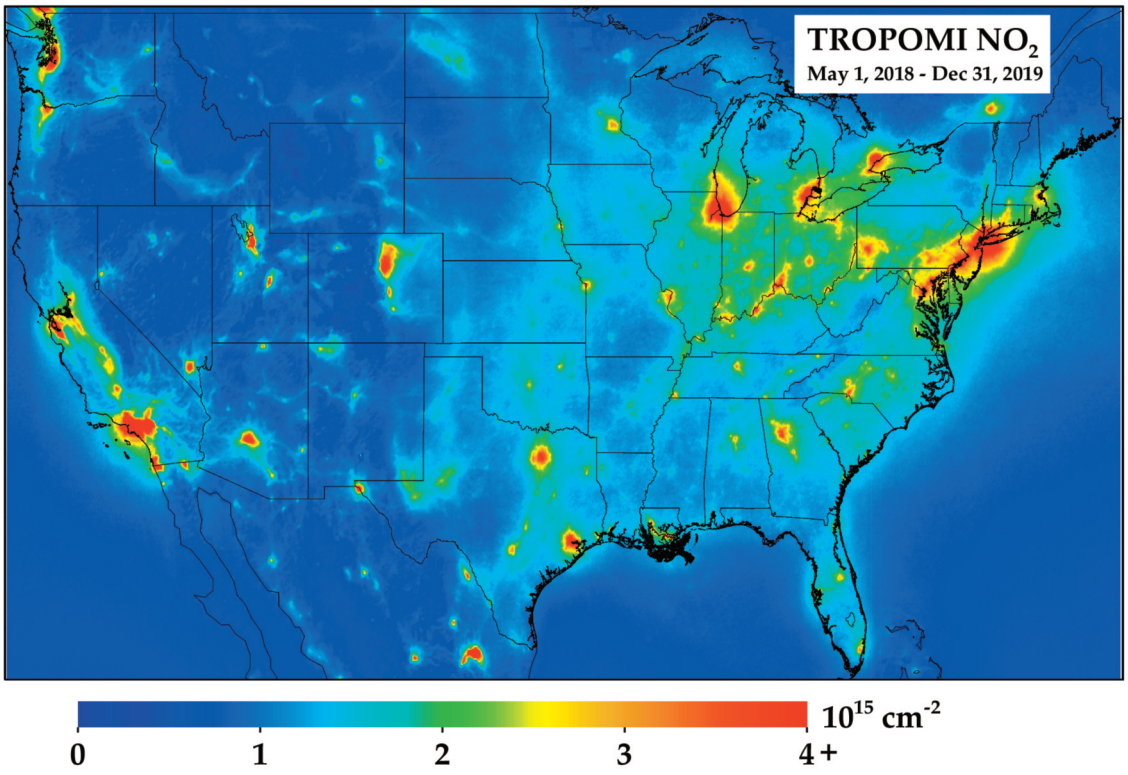

Figure 1. TROPOMI NO_2 oversampled to 0.01° × 0.01° spatial resolution during May 1, 2018–December 31, 2019. Only pixels exceeding a quality assurance flag of 0.75 are included.

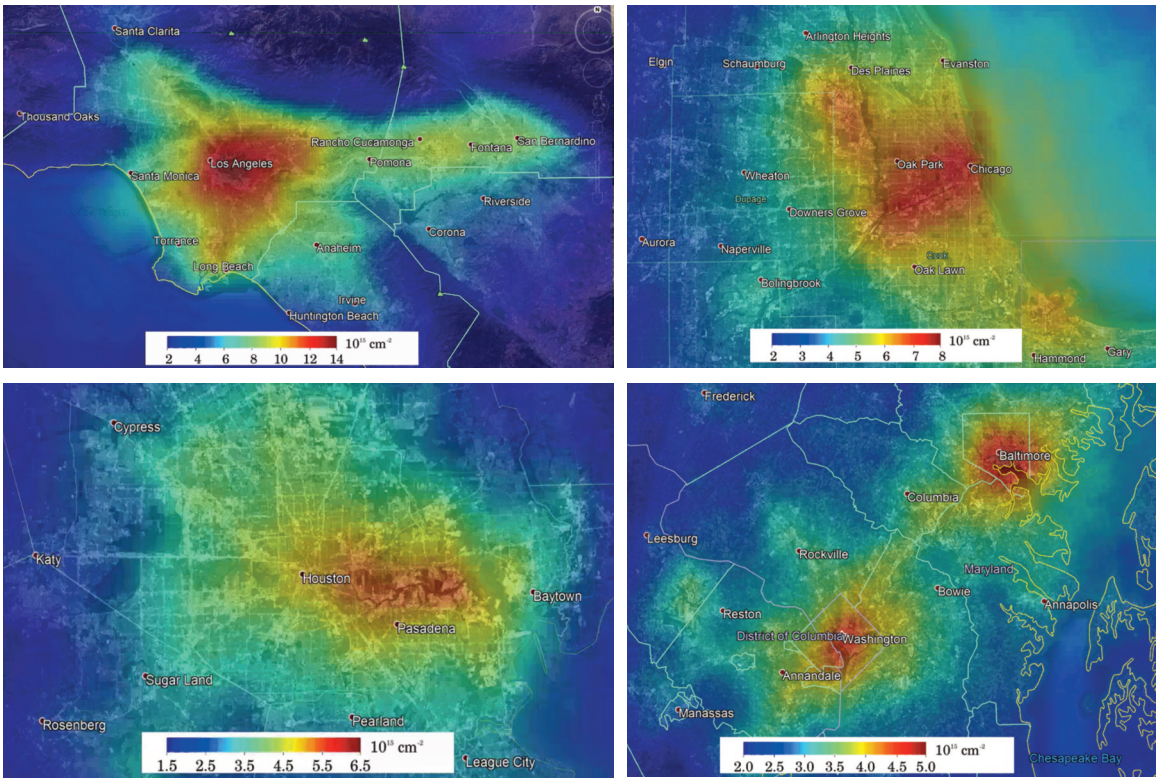

Figure 2. Same data shown in Figure 1, but now zoomed into four different U.S. cities (clockwise from top left: Los Angeles, Chicago, Washington DC/Baltimore corridor, and Houston). Color bar has been adjusted to better differentiate spatial heterogeneity on a local scale.

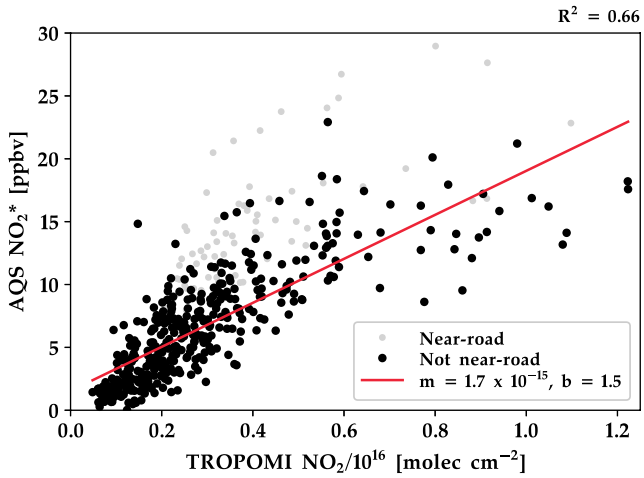

Figure 3. EPA AQS annual surface NO2* observations for 2019 compared to the collocated oversampled 0.01° × 0.01° TROPOMI value during the same timeframe.

Equally important, relatively smaller sources of NO_2 pollution can now be observed, and they are not spatially smeared into the background NO_2 concentration. For example, the roadway network and related activity in the Idaho Snake River valley can be clearly observed. Individual spikes in NO_2 associated with NOx emissions from large power plants (e.g., Colstrip in Montana, Hunter/Huntington in Utah) can also be observed during this 2018–2019 period even though there have been large reductions (~85%) in the NOx emissions from large power plants since the introduction of the federally mandated NOx SIP Call in 2003. Other examples are the metal mining operations in Nevada and Arizona, the coal mining operations in the Powder River and Green River Basins in Wyoming, and oil and gas operations in the Permian (Texas) and Bakken (North Dakota) Basins.

TROPOMI data are especially powerful in analyzing local variations in NO_2 pollution as compared to predecessor instruments. Figure 2 zooms into four different U.S. metropolitan areas. In each instance, the oversampled TROPOMI NO_2 images exhibit features that match known NOx emissions patterns. Larger NO_2 values can be seen around the interstate network, population density, and industrial activity hubs (e.g., manufacturing facilities, airports, and shipping ports).

For example, in Los Angeles, the spatial pattern matches the basin outline very well, with the largest values between

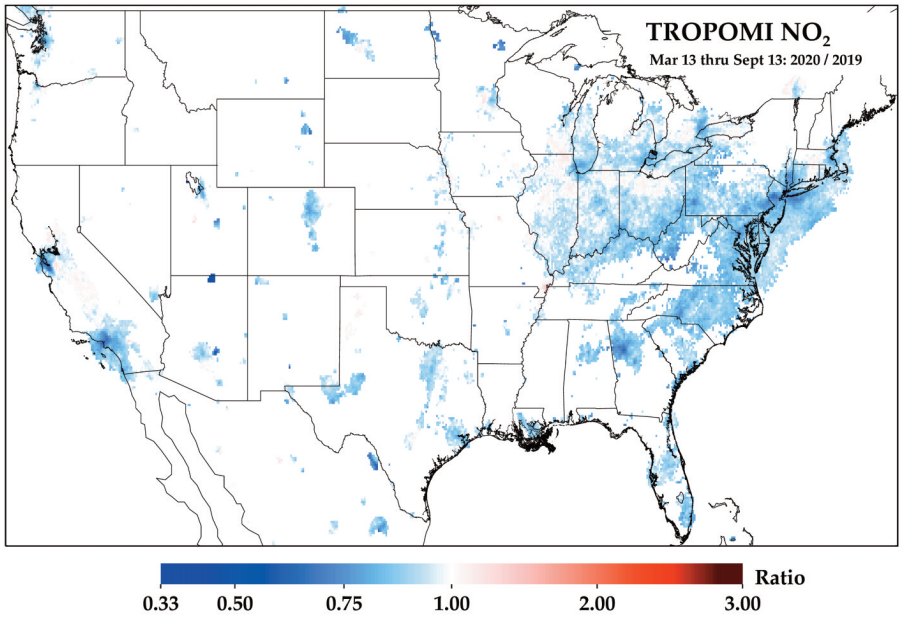

City	Changes
San Jose:	-33.6%
Los Angeles:	-30.0%
New York City:	-26.7%
Atlanta:	-26.5%
Boston:	-24.7%
Washington DC:	-24.5%
Philadelphia:	-21.5%
Toronto:	-20.4%
Seattle:	-19.5%
Chicago:	-18.7%
Detroit:	-17.1%
Denver:	-16.7%
Houston:	-16.4%
Miami:	-15.3%
Phoenix:	-13.1%
Minneapolis:	-12.6%
San Francisco:	-12.4%
Las Vegas:	-11.8%
Vancouver:	-10.4%
Portland:	-10.1%
Austin:	-8.8%
Dallas:	-7.9%
New Orleans:	-1.7%

Figure 4. Differences in column NO_2 between March 13, 2020, and Sept 13, 2020, and the coincident timeframe in 2019, reported as a ratio. Locations with values less than 1.5 x 1015 molec/cm^2 in 2019 have been screened out due to the strong effects of natural variability in these locations. NO_2 changes in 23 North American urban areas during the timeframe are displayed in the accompanying table.

downtown Los Angeles and the Long Beach Shipping Port. The largest values in Chicago exist along the I-55 corridor, which has a high traffic volume and a high density of industrial facilities, with secondary maxima at the O'Hare International airport and the U.S. Steel Corp operations in East Chicago, Indiana. In the image of Maryland and Washington DC, the largest value is observed at the Baltimore Harbor, which has a confluence of several major highways, a large shipping port, the city incinerator, and many industrial facilities. In Houston, Texas the largest values are nearest to the petrochemical refining facilities east of town.

In all cases, TROPOMI captures the collocation of the largest sources of NOx emissions and NO_2 concentrations. For this reason, TROPOMI observations can be a valuable way to evaluate the fine-scale structure of NO_2 concentrations in environmental justice communities.[11-13]

Relationship with Surface Monitor NO_2 Concentrations

To understand how well TROPOMI, without any adjustment, captures surface-level NO_2 concentrations, we compare the 2019 annual TROPOMI NO_2 average to 24-hr annual average surface NO_2 concentrations from the U.S. Environmental Protection Agency (EPA) Air Quality System (AQS) monitor network. Figure 3 shows a scatterplot between 2019 annual averages of oversampled TROPOMI NO_2 and AQS surface-level NO_2* (surface-level concentrations from the EPA AQS network are known to have a high instrument bias that varies spatiotemporally,[14,15] and are thus referred here to as NO_2*).

Figure 3 demonstrates that there is a strong correlation (R2 = 0.66) between TROPOMI NO_2 values and surface NO_2* observations at monitoring sites considered to be not within 20 m of a roadway (i.e., "not near-road"), which suggests that many (but not all) of the spatial heterogeneities observed by TROPOMI over long time intervals (e.g., year) are real and not an artifact of the processing algorithms. To better estimate surface-level concentrations, TROPOMI NO_2 data should be merged with a model simulation[16] and/or land-use characteristics.[17-20]

Case Study: Changes due to the COVID-19 Lockdowns

In Figure 4, we use TROPOMI NO_2 to quantify the NO_2 changes in the continental United States and southern Canada due to the COVID-19 pandemic lockdowns. TROPOMI is an advantageous tool in this instance due to its global spatial coverage and the rapid availability of observations in a consistent data format transcending the borders of all countries. We compare the TROPOMI NO_2 mean of the first six months of the COVID lockdowns (March 13, 2020–September 13, 2020) to the coincident timeframe of 2019 in order to account for the effects of seasonality and meteorology on NO_2 concentrations.[21] Because we compare over a

six-month period, it is reasonable to assume that the majority of the NO_2 changes are due to NOx emissions changes.

The largest NO_2 decreases due to the lockdowns were seen in California (San Jose and Los Angeles) and the major cities of the eastern United States (New York City, Washington, DC, Atlanta, and Boston). Conversely, the cities in the central United States documented smaller NO_2 changes (Dallas, Austin, New Orleans, and Minneapolis). We also observe substantial NO_2 decreases near the retired Navajo power plant in northern Arizona. Areas with small NO_2 have been screened due to the high fraction of NO_2 attributed to biogenic sources and long-range transport.

Conclusion

This article describes the capabilities of TROPOMI in observing the spatial and temporal patterns of NO_2 pollution in the Continental United States. TROPOMI has unprecedented spatial resolution that allows it to quantify the fine-scale patterns of NOx emissions that had previously been reported at coarser resolution or in some cases had gone completely undetected from space-based instruments. Furthermore, due to the instrument's excellent stability, precision, and spatial resolution, it is no longer necessary to average over 6+ months of data to gain a clear depiction of regional NO_2 abundances; instead, monthly, weekly, or even daily aggregations could suffice for many purposes.

The examples presented here demonstrate how TROPOMI NO_2 satellite data can be advantageous for assessing, designing, and evaluating regulations and other factors influencing emission changes. Future health impact assessment studies can use the high-spatial resolution capabilities of TROPOMI NO_2 to investigate disparities in traffic-related air pollution exposure and associated health effects between neighborhoods and population sub-groups within cities. **em**

Daniel L. Goldberg, Susan C. Anenberg and **Gaige Hunter Kerr** are all with the Department of Environmental and Occupational Health, George Washington University, Washington, DC. **Zifeng Lu** and **David G. Streets** are both with the Energy Systems Division, Argonne National Laboratory. E-mail: **dgoldberg@gwu.edu**.

References

1. Burns, D.A.; Gay, D.A.; Lehmann, C.M.B. Acid rain and its environmental effects: Recent scientific advances; *Atmos. Environ.* 2016, *146*, 1-4; https://doi.org/10.1016/J.ATMOSENV.2016.10.019.
2. Broeckaert, F.; Arsalane, K.; Hermans, C.; Bergamaschi, E.; Brustolin, A.; Mutti, A.; Bernard, A. Lung epithelial damage at low concentrations of ambient ozone; *The Lancet* 1999, *353* (9156), 900-901; https://doi.org/10.1016/S0140-6736(99)00540-1.
3. McConnell, R.; Berhane, K.; Gilliland, F.; London, S.J.; Islam, T.; Gauderman, W.J., et al. Asthma in exercising children exposed to ozone: a cohort study; *The Lancet* 2002, *359* (9304), 386-391; https://doi.org/10.1016/S0140-6736(02)07597-9.
4. Burnett, R.T.; Stieb, D.; Brook, J.R.; Cakmak, S.; Dales, R.; Raizenne, M., et al. Associations between short-term changes in nitrogen dioxide and mortality in Canadian cities; *Archives of Environmental Health* 2004, *59* (5), 228-236; https://doi.org/10.3200/AEOH.59.5.228-236.
5. van Geffen, J.; Boersma, K.F.; Eskes, H.; Sneep, M.; ter Linden, M.; Zara, M.; Veefkind, J.P. S5P TROPOMI NO_2 slant column retrieval: method, stability, uncertainties, and comparisons with OMI; *Atmospheric Measurement Techniques* 2020, *13* (3), 1315-1335; https://doi.org/10.5194/amt-13-1315-2020.
6. Veefkind, J.P.; Aben, I.; McMullan, K.; Förster, H.; de Vries, J.; Otter, G., et al. TROPOMI on the ESA Sentinel-5 Precursor: A GMES mission for global observations of the atmospheric composition for climate, air quality, and ozone layer applications; *Remote Sensing of Environment* 2012, *120* (2012), 70-83; https://doi.org/10.1016/j.rse.2011.09.027.
7. Sun, K.; Zhu, L.; Cady-Pereira, K.E.; Chan Miller, C.; Chance, K.V.; Clarisse, L., et al. A physics-based approach to oversample multi-satellite, multi-species observations to a common grid; *Atmospheric Measurement Techniques Discussions* 2018, *11* (12), 1-30; https://doi.org/10.5194/amt-2018-253.
8. Levelt, P.F.; Joiner, J.; Tamminen, J.; Veefkind, J.P.; Bhartia, P.K.; Zweers, D.C.S., et al. The Ozone Monitoring Instrument: Overview of 14 years in space; *Atmospheric Chemistry and Physics* 2018, *18* (8), 5699-5745; https://doi.org/10.5194/acp-18-5699-2018.
9. Burrows, J.P.; Weber, M.; Buchwitz, M.; Rozanov, V.; Ladstatter-Weibenmayer, A.; Richter, A., et al. The Global Ozone Monitoring Experiment (GOME): Mission Concept and First Scientific Results; *Journal of Atmospheric Sciences* 1999, *56*, 151-175; https://doi.org/10.1175/1520-0469(1999)056<0151:TGOMEG>2.0.CO;2.
10. Goldberg, D.L.; Anenberg, S.C.; Kerr, G.H.; Mohegh, A.; Lu, Z.; Streets, D.G. TROPOMI NO_2 in the United States: A detailed look at the annual averages, weekly cycles, effects of temperature, and correlation with surface NO2 concentrations; *Earth's Future* 2021, e2020EF001665; https://doi.org/10.1029/2020EF001665.
11. Anenberg, S.; Kerr, G.H.; Goldberg, D.L. Leveraging satellite data to address air pollution inequities; *EM*, September 2021.
12. Demetillo, M.A.G.; Navarro, A.; Knowles, K.K.; Fields, K.P.; Geddes, J.A.; Nowlan, C.R., et al. Observing Nitrogen Dioxide Air Pollution Inequality Using High-Spatial-Resolution Remote Sensing Measurements in Houston, Texas; *Environ. Sci. Technol.* 2020, acs.est.0c01864; https://doi.org/10.1021/acs.est.0c01864.
13. Kerr, G.H.; Goldberg, D.L.; Anenberg, S. COVID-19 pandemic reveals persistent disparities in nitrogen dioxide pollution; *ESSOAr: Earth and Space Science Open Archive*, 2021; https://doi.org/10.1002/ESSOAR.10504561.3.
14. Dickerson, R.R.; Anderson, D.C.; Ren, X. On the use of data from commercial NOx analyzers for air pollution studies; *Atmos. Environ.* 2019, 116873; https://doi.org/10.1016/j.atmosenv.2019.116873.
15. Lamsal, L.N.; Martin, R.V.; van Donkelaar, A.; Steinbacher, M.; Celarier, E.A.; Bucsela, E.J., et al. Ground-level nitrogen dioxide concentrations inferred from the satellite-borne Ozone Monitoring Instrument; *Journal of Geophysical Research Atmospheres* 2008, *113* (16), 1-15; https://doi.org/10.1029/2007JD009235.
16. Cooper, M.J.; Martin, R.V.; McLinden, C.A.; Brook, J.R. Inferring ground-level nitrogen dioxide concentrations at fine spatial resolution applied to the TROPOMI satellite instrument; *Environ. Res. Letts.* 2020; https://doi.org/10.1088/1748-9326/aba3a5.
17. Bechle, M.J.; Millet, D.B.; Marshall, J.D. National Spatiotemporal Exposure Surface for NO_2: Monthly Scaling of a Satellite-Derived Land-Use Regression, 2000-2010; *Environ. Sci. Technol.* 2015, *49* (20), 12297-12305; https://doi.org/10.1021/acs.est.5b02882.
18. Beloconi, A.; Vounatsou, P. Bayesian geostatistical modelling of high-resolution NO_2 exposure in Europe combining data from monitors, satellites, and chemical transport models; *Environment International* 2020, *138*, 105578; https://doi.org/10.1016/j.envint.2020.105578.
19. Di, Q.; Amini, H.; Shi, L.; Kloog, I.; Silvern, R.F.; Kelly, J.T., et al. Assessing NO_2 Concentration and Model Uncertainty with High Spatiotemporal Resolution across the Contiguous United States Using Ensemble Model Averaging; *Environ. Sci. Technol.* 2019, acs.est.9b03358; https://doi.org/10.1021/acs.est.9b03358.
20. Larkin, A.; Geddes, J.A.; Martin, R.V.; Xiao, Q.; Liu, Y.; Marshall, J.D., et al. Global Land Use Regression Model for Nitrogen Dioxide Air Pollution; *Environ. Sci. Technol.* 2017, *51* (12), 6957-6964; https://doi.org/10.1021/acs.est.7b01148.
21. Goldberg, D.L.; Anenberg, S.C.; Griffin, D.; McLinden, C.A.; Lu, Z.; Streets, D.G. Disentangling the Impact of the COVID−19 Lockdowns on Urban NO2 From Natural Variability; *Geophys. Res. Letts.* 2020, *47* (17); https://doi.org/10.1029/2020GL089269.